

Change of Scaling and Appearance of Scale-Free Size Distribution in Aggregation Kinetics by Additive Rules

Yuri G. Gordienko

*G.V.Kurdyumov Institute for Metal Physics, National Academy of Sciences of Ukraine,
36 Academician Vernadsky Blvd, Kiev 03680, Ukraine*

Abstract

Recently several models and theories were proposed to describe and explain the scale-invariant behavior of crystal defect aggregations that possibly lead to self-affine geometry of fractured surfaces. Here the idealized general model of aggregate growth is proposed on the basis of the simple additive rules that correspond to one-step aggregation process. Some factors that can influence the self-affine nature of the aggregating system of solitary agents (monomers) and their aggregates (clusters) were brought to light: the rate of monomer particle exchange between clusters, cluster geometry, and initial cluster size. Two idealized cases were analytically investigated and simulated by Monte Carlo method in the Desktop Grid distributed computing environment to analyze “pile-up” and “wall” cluster distributions in different aggregation scenarios. The “pile-up” case with a *minimum* active surface (singularity) could imitate piling up aggregations of dislocations, and the case with a *maximum* active surface could imitate arrangements of dislocations in walls. The change of scaling law (for pile-ups and walls) and availability of scale-free distributions (for walls) were analytically shown and confirmed by scaling analysis of simulated density and cumulative density distributions. The initial “singular” *symmetric* distribution of pile-ups evolves by the “infinite” diffusive scaling law and later it is replaced by the other “semi-infinite” diffusive scaling law with *asymmetric* distribution of pile-ups. In contrast, the initial “singular” *symmetric* distributions of walls initially evolve by the diffusive scaling law and later it is replaced by the other linear scaling law with *scale-free* exponential distributions without distinctive peaks. The conclusion was made as to possible applications of such approach for scaling analysis of cumulative density distributions in experimental data.

Keywords: aggregation kinetics, stochastic process, one-step process, Fokker-Planck equation, scaling, scale-free distributions, crystal lattice defects, desktop grid

1. Introduction

In materials science the fractured surfaces demonstrate the self-affine geometry on many scales. Moreover, the fractal analysis of fractured surfaces by projective covering and box-counting method shows that the fractured surface can be depicted not only by one fractal dimension, but also by multifractal spectrum [1, 2]. At the same time, surface roughness profiles of periodically deformed Al [3, 4, 5], slip line morphology in Cu [6, 7], and dislocation patterns in Cu after tensile [8] also demonstrate the self-similar features on many scales. Recently, transition from homogeneous dislocation arrangement to scale-invariant structure was described by the statistical model of noise-induced transition [9]. Several other models and theories were proposed to explain the scale-invariant behavior of crystal defect aggregations that possibly lead to self-affine geometry of fractured surfaces [10].

The hierarchical defect substructures that were observed experimentally in deformed metals and alloys appear as a result of some aggregation processes among solitary crystal defects. It should be noted that many aggregation phenomena in other natural processes also take place by exchange of solitary agents (monomers) between their aggregates (clusters): phase ordering [11, 12], atom deposition [13], stellar evolution [14], growth and distribution of assets [15], and city population even [16]. In such aggregation processes monomers can leave one cluster and attach to another. Usually these exchange processes are described by an exchange rate kernel $K(i, j)$, i.e. by the rate of transfer of monomers from a cluster of size i (detaching event) to a cluster of size j (attaching event). Generally, the rate of monomer exchange between two clusters depends on their active interface surfaces that are dependent on their sizes, morphology (line, plane, disk, sphere, fractal, etc), probability of detaching and attaching events, etc.

Sometimes there is the preferable direction for exchanges, i.e. with asymmetric exchange kernels, $K(i, j) \neq K(j, i)$, like in coalescence processes in Lifshitz-Slyozov-Wagner theory [11, 12], where big clusters “eat” smaller ones. The exchange rate kernel $K(i, j)$ is defined by the product of the rate at which monomer detach from a cluster of size i and the rate at which this

monomer reach another cluster of size j . In Leyvraz-Redner scaling theory of aggregate growth [16] cities A_i of size i evolve according to the following rule:

$$A_i + A_j \xrightarrow{K(i;j)} A_{i-1} + A_{j+1}, \quad (1)$$

where $K(i, j)$ is the exchange rate. That is, monomer (one person) leaves some of cities A_i of population i and arrive to some of cities A_j of population j . This can be considered as the generalized rule for the theory of growth and distribution of assets [15], if one can assume that A_i are persons with asset volume of i .

Below the idealized general model of aggregate growth is proposed on the basis of this approach. The main aim of the work is to use the most profound features of aggregation kinetics and to find the simplest factors that can cause the observed self-affine properties of the aggregating system of solitary agents (monomers) and their aggregates (clusters). In this context, the numerous complex details of the real crystal defect aggregation processes will be hidden behind the idealized and simplified conditions only to emphasize the most general precursors of scale-invariant behavior of such complex systems.

2. Model

Here detaching and attaching processes are considered separately that in the general case could be characterized by different rates. Consequently, the different detach product kernel $K_d(n) = k_d S(n)$ and attach product kernel $K_a(n) = k_a S_a(n)$ are taken into account, where k_d and k_a are the measures of activation of detaching and attaching processes, n is the number of monomers in a cluster. In natural processes k_d is usually determined by energy barrier for detachment from cluster and k_a — by probability for attachment of migrating monomer to another cluster which in turn determined by kind of migration (instant hops from cluster to cluster, ballistic motion, random walking, or their combinations). $S_d(n) = s_d n^\alpha$ and $S_a(n) = s_a n^\beta$ are the active surfaces of clusters, where α and β — exponents depending on the morphology of cluster (for example $\alpha = 1$ for linear clusters and $\alpha = 2/3$ for spherical clusters, and $\alpha = \beta$ in the simplest case of clusters with the same morphology), s_d and s_a — the constants depending on the morphology of cluster and geometry of neighborhood (for example $s_d = 1$ for linear aggregates and $s_d = \sqrt[3]{36\pi}$ for spherical aggregates, and $s_d = s_a = s$ in the

simplest case of clusters with the same morphology and neighborhood). The portion of clusters $f(n, t)$ with n monomers at time t evolves according to the following equation:

$$\begin{aligned} \frac{\partial f(n, t)}{\partial t} = & K_d(n+1)f(n+1, t) + K_a(n-1)f(n-1, t) - \\ & - K_d(n)f(n, t) - K_a(n)f(n, t) \end{aligned} \quad (2)$$

Actually this is the well-known master equation for so-called “one-step process”, i.e. a continuous time stochastic Markov process, which range consists of integer n , and where transitions allowed only between adjacent integers [17].

The general model is based on the assumption that the migration time (movement of a monomer from one cluster to other) is much lower than the detachment (or attachment) time of a monomer from (to) a cluster. That is why there are no free monomers, and range of n is half-infinite ($n = 2, 3, \dots$). At the same time the total number of monomers is assumed to be constant and no generation sources exist. It should be taken into account that the more consistent system of evolution equations and more realistic coupling between migration and detachment (attachment) times should be used for rigorous comparison of this general model and each case of the aforementioned natural processes.

In an asymptotic regime of high values of n equation (2) goes to:

$$\frac{\partial f(n, t)}{\partial t} \approx \frac{\partial (D_1(n) f(n, t))}{\partial n} + \frac{\partial^2 (D_2(n) f(n, t))}{\partial n^2}, \quad (3)$$

which is the one-variable Fokker-Planck equation in general form with time-independent drift $D_1(n) = K_d(n) - K_a(n) = n^\alpha s (k_d - k_a)$ and diffusion $D_2(n) = K_a(n) = n^\alpha s k_a$ coefficients [18, 19]. The main difference between this formulation and other well-known models is the more general scenario with detaching and attaching as separate events is taken into account here. It allows us to express explicitly the availability of drift and diffusion terms, and, moreover, to bring to light the common symmetry properties and propose the ways to find the exact non-stationary solutions [20].

The case $\alpha = 0$ corresponds to the clusters with the minimum active surface (“singularity” of the active surface), namely for clusters with constant numbers of active monomers independent of the whole number of monomers n in it. For example, the ends of a line cluster can be its 2 active points

for detaching and attaching. Such configurations take place in queues (2 active points), stacks (1 active point), etc. In the context of plastic deformation of metals, “pile-up” aggregations of dislocations of a regular crystalline structure can be depicted by this scenario (see Fig. 1a).

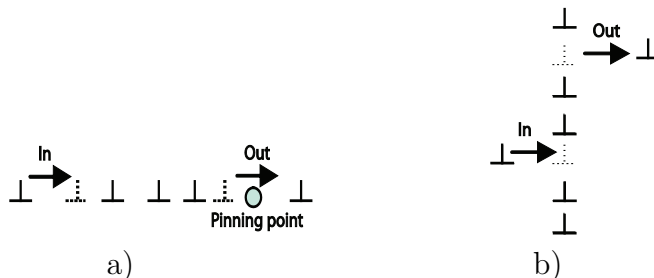


Figure 1: Examples of (a) minimum active surface — pile-up of dislocations: it is possible to go in/out pile-up only through left/right ends of the pile-up; and (b) maximum active surface — wall of dislocations: it is possible to go in/out wall in any place.

The case $\alpha = 1$ corresponds to the clusters with the maximum active surface, namely for clusters where any monomer could be detached and free monomer could be attached to any place. Again, in plastically deformed metals, “wall” aggregations of dislocations of a regular crystalline structure can be depicted by this scenario (see Fig. 1b). In Leyvraz-Redner scaling theory of aggregate growth of city population [16] it can correspond to linear dependence of arrival or departure rates as a function of city population.

The case $0 < \alpha < 1$ corresponds to the clusters with the bulk volume of monomers shielded by active surface. For example, circumference of disk, perimeter of fractal, outer layer of sphere can be the correspondent active surfaces for detaching and attaching. In solid state physics, such configurations take place in regular arrangements (compact like voids and sparse like fractals) of point-like defects of a crystalline structure.

The case $k_d = k_a$ corresponds to the equiprobable activation of detaching and attaching processes, for example, for periodic tensile deformation it can correspond to the equiprobable activation of detaching and attaching dislocations from opposite sides of wall. Finally, it means the absence of the drift term in (3).

2.1. Pile-up - minimum active surface

For the case $\alpha = 0$ clusters have the minimum active surface and under condition $k_d = k_a$ one can get the well-known heat equation, where $a = sk_a$,

$$\frac{\partial f(n, t)}{\partial t} = a \frac{\partial^2 f(n, t)}{\partial n^2}, \quad (4)$$

which has numerous particular solutions that are dependent on the initial and boundary conditions. In the reality $k_d \neq k_a$, and the aggregation process is described by the homogeneous heat equation with space-independent drift and diffusion coefficients. It is well-known fact that it leads to “a diffusive-like kinetic universality class”.

Below for illustrative purpose we consider the time evolution of the initial singular distribution of clusters of the same size (n_0) that exchange the monomers. It is actually the first boundary value problem for domain $0 < n < \infty$, $f(0, t) = 0$, $f(n, 0) = \delta(n - n_0)$, where $\delta(n)$ is a Dirac delta function. This problem has the well-known solution:

$$f(n, t) = \frac{1}{2\sqrt{\pi at}} \left\{ \exp \left[-\frac{(n - n_0)^2}{4at} \right] - \exp \left[-\frac{(n + n_0)^2}{4at} \right] \right\}. \quad (5)$$

In practice, $f(n, t)$ could be experimentally determined for high values of n and t . That is why $f(n, t)$ is of interest for large values of $n \gg n_0$ and $t \gg n^2/4a$:

$$f(n, t) = \frac{nn_0}{2\sqrt{\pi} (at)^{3/2}} \exp \left[-\frac{n^2}{4at} \right]. \quad (6)$$

The essential point is that on the initial stage of this one-step aggregation process the probability distribution function $f(n, t)$ does not “feel” the boundary condition $f(0, t) = 0$. From the physical point of view the cluster size cannot reach the 0-boundary (and equation cannot “feel” the boundary condition) immediately, but only after some time t_0 , when the first cluster disappear due to detaching monomers. It means that on the initial stage $t < t_0$ the aforementioned problem formulated as the classic Cauchy problem for *infinite* domain $-\infty < n < \infty$ with the same initial condition $f(n, 0) = \delta(n - n_0)$ and the well-known solution:

$$f_{t < t_0}(n, t) = \frac{1}{2\sqrt{\pi at}} \exp \left[-\frac{(n - n_0)^2}{4at} \right] \quad (7)$$

and for $n \gg n_0$ it goes to the following shape:

$$f_{t < t_0}(n, t) \rightarrow \frac{1}{2\sqrt{\pi at}} \exp\left[-\frac{n^2}{4at}\right]. \quad (8)$$

Thus we have two different scaling laws for the probability distribution functions for pile-ups $f(n, t)$ for high values of $n \gg n_0$:

- for $t < t_0$ (“infinite” diffusive scaling law)

$$f_{t < t_0}(n, \lambda t) \rightarrow \lambda^{-1/2} f(\lambda^{-1/2} n, t), \quad (9)$$

- for $t > t_0$ (“semi-infinite” diffusive scaling law)

$$f_{t > t_0}(n, \lambda t) \rightarrow \lambda^{-1} f(\lambda^{-1/2} n, t). \quad (10)$$

From practical point of view it is not easy to distinguish scaling laws (9) and (10) and difference between them by analysis of probability density functions $f(n)$ for various moments of time (Fig. 2a), especially from scarce and noisy experimental data.

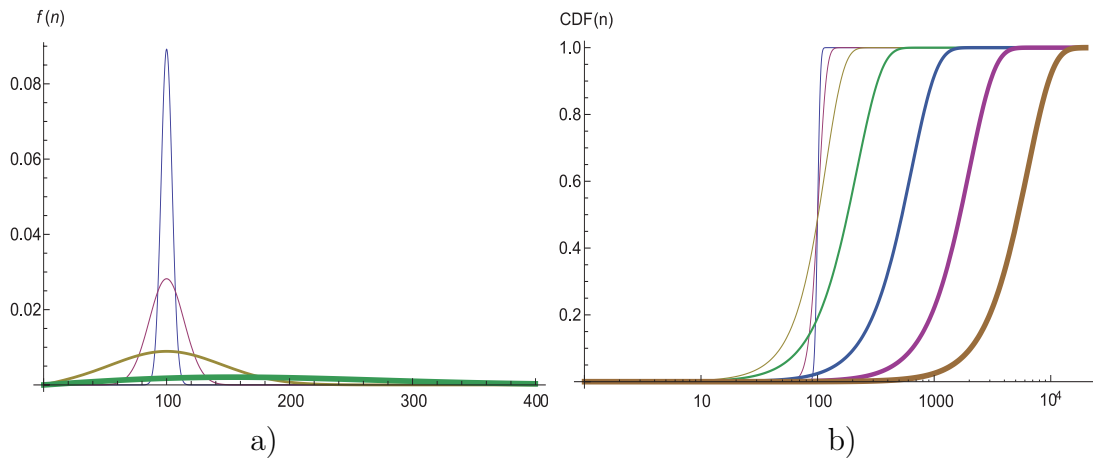


Figure 2: Pile-up size distributions: probability density functions $f(n)$ (a) and their cumulative distribution functions $CDF(n)$ (b) for different stages of aggregation kinetics (4). Thickness of lines corresponds to the increasing values of t in the order from the thinnest to thickest line: (a) 100; 1000; 2000; 4000; and (b) 10; 10^2 ; 10^3 ; 10^4 ; 10^5 ; 10^6 ; 10^7 .

But it is much more easier to observe the scaling laws by analysis of the cumulative distribution functions. For example, the visual comprehension of

scaling law (10) can be easily obtained by viewing the steady shift of the correspondent cumulative distribution functions (CDFs) to the right side in Fig. 2b. The shift becomes diffusive (i.e. proportional to \sqrt{t}) after $t > 10^4$, when the first cluster will reach the 0-boundary, i.e. by continuous detachments some cluster will decrease its size to 0 and disappear.

It means that one can determine the qualitatively different scaling regimes — “infinite” (9) and “semi-infinite” (10) — in this aggregation model with additive rules by the scaling analysis of the probability distribution function $f(n, t)$ for high values of $n \gg n_0$. As it will be shown below in section 4, scaling analysis of cumulative density functions is more efficient for practical purposes. The unbounded case (Cauchy problem for infinite domain $-\infty < n < \infty$) corresponds to a situation with the constant number of clusters (monomers only redistribute between them), and the bounded one (first boundary value problem for domain $0 \leq n < \infty$) — to a situation with irreversible decrease of the number of clusters.

2.2. Wall - maximum active surface

For the case $\alpha = 1$ clusters have the minimum active surface and under condition $k_d = k_a$ one can get:

$$\frac{\partial f(n, t)}{\partial t} = a \frac{\partial^2 (n f(n, t))}{\partial n^2}, \quad (11)$$

which has numerous particular solutions $f(n, t) \sim F(n/t)$ that are dependent on the initial and boundary conditions. Again for illustrative purpose we consider the time evolution of the initial singular distribution of clusters of the same size (n_0) that exchange the monomers. It is actually the first boundary value problem for domain $0 \leq n < \infty$, $f(0, t) = 0$, $f(n, 0) = \delta(n - n_0)$ with the following solution:

$$f(n, t) = \frac{\sqrt{n_0}}{at\sqrt{n}} \exp\left[-\frac{(n + n_0)}{at}\right] I_1\left(\frac{2\sqrt{nn_0}}{at}\right). \quad (12)$$

Again, on the initial stage of this one-step aggregation process the probability distribution function $f(n, t)$ does not “feel” the boundary condition $f(0, t) = 0$, because from the physical point of view the cluster size cannot reach the boundary immediately, but only after some time t_0 , when the first cluster disappear due to detaching monomers. When $t \ll t_0$ and $n \approx n_0$, the solution of (11) has not influenced by differences in n significantly and

that is why it has approximate solution, which is close to solution of the heat equation:

$$f_{t < t_0}(n, t) \rightarrow \frac{1}{2\sqrt{\pi at}} \exp\left[-\frac{n^2}{4at}\right]. \quad (13)$$

But for the later stage $t > t_0$ solution of (11) will be close to:

$$f_{t > t_0}(n, t) \rightarrow \frac{\sqrt{n_0}}{at\sqrt{n}} \exp\left[-\frac{n}{at}\right] I_1\left(\frac{2\sqrt{nn_0}}{at}\right) \quad (14)$$

and for $n \gg n_0$ it goes to the following shape:

$$f_{t > t_0}(n, t) \rightarrow \frac{n_0}{a^2 t^2} \exp\left[-\frac{n}{at}\right]. \quad (15)$$

Thus, again we have two different scaling laws for the probability distribution function of walls $f(n, t)$ for $n \gg n_0$:

- for $t < t_0$ (“infinite” diffusive scaling law)

$$f_{t < t_0}(n, \lambda t) \rightarrow \lambda^{-1/2} f(\lambda^{-1/2} n, t), \quad (16)$$

- for $t > t_0$ and $n \gg n_0$ (“semi-infinite” linear scaling law)

$$f_{t > t_0}(n, \lambda t) \rightarrow \lambda^{-2} f(\lambda n, \lambda t). \quad (17)$$

Again, as in the case with pile-ups, it is not easy to distinguish scaling laws (16) and (17) and difference between them by analysis of probability density functions $f(n)$ for various moments of time (Fig. 3a), especially from experimental data.

And it is much more easier to observe the scaling laws by analysis of the cumulative distribution functions (Fig. 3b). The visual comprehension of scaling law (17) can be easily obtained by viewing the steady shift of the cumulative distribution functions (CDFs) to the right side in Fig. 3b. The shift becomes linear (i.e. proportional to t) after $t > 10^2$ (but not after $t > 10^4$, like it was for pile-ups!), when the first cluster will reach the 0-boundary, i.e. when some cluster by continuous detachments will decrease its size to 0 and disappear. But the most essential point is that shortly after $t > t_0$ the size distribution for wall configuration becomes exponential (15), that is scale-free one and without any “apparent” peak value.

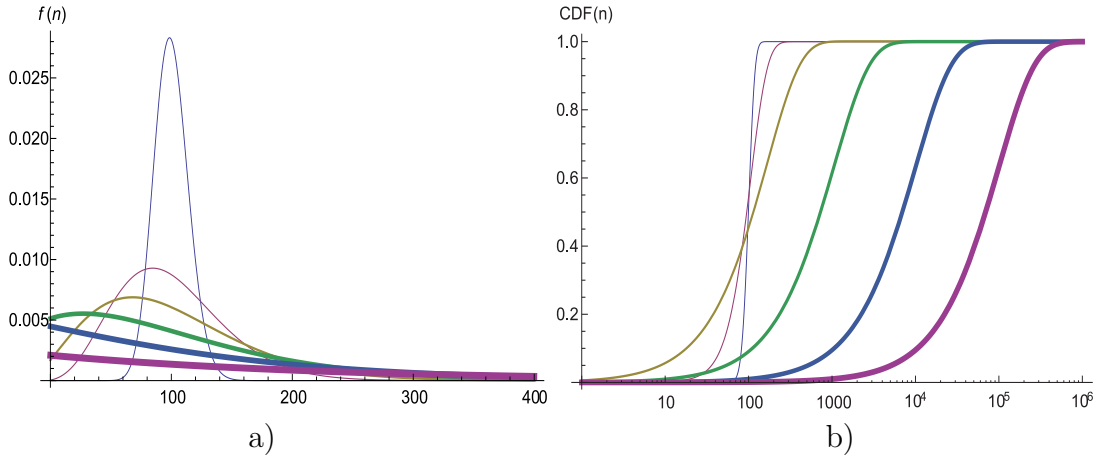


Figure 3: Wall size distributions for different stages of aggregation kinetics (a) and their cumulative distribution functions (b). Thickness of lines corresponds to the values of t in the order from the thickest to thinnest line: (a) 1; 10; 20; 40; 80; 160; and (b) 1; 10; 10^2 ; 10^3 ; 10^4 ; 10^5

One of drawbacks of the simplified model is that the equations (4) and (11) and their solutions (5) and (12) give the idealized and rough representation of the aggregation kinetics. In fact, solutions (5) and (12) allows the “long-tails” of distribution, i.e. non-zero density of clusters for arbitrary high or low values of n in the ranges $n > n_0$ and $n < n_0$ for any stage of evolution. For example, any initial cluster of size $n = 10^2$ will need at least $t = 10^2$ detachment steps to disappear. But the analytical solution (5) gives the non-zero values of cluster distribution $f(n, t)$ for any small n , i.e. does not prohibit immediate disappearance of this initial cluster even at the first step after start of the aggregation process. In a real physical process it is impossible due to physical limitations of diffusive character of the one-step aggregation process among clusters with pile-up morphology. This situation is well-known and actively investigated in the class of so-called “first-passage problems” [17]. That is why, the analytical solutions and predictions of the model cannot be directly applied to the correspondent practical situations without taking into account the limits of their physical counterparts. Here, we investigated the aforementioned scaling laws and transitions between them by the following simulations.

3. Simulation

The two aforementioned primitive cases of cluster aggregation were simulated by Monte Carlo method to illustrate the different cluster distributions in different aggregation kinetics. The numerous initial configurations of clusters with various numbers of monomers in each of them were used in simulations with a conserved number of 10^6 aggregating monomers as a whole. Below the results on initial configurations of 10^4 clusters with 10^2 monomers are considered (and the other vast configurations will be reported later [20]). Further the analytical calculations in section 2 will be compared with the results of simulation and for this purpose the number of MCSs will be assumed to equal to the number of time steps t . All simulation runs were performed in the distributed computing infrastructure (DCI) “SLinCA@Home” (Scaling Law in Cluster Aggregation) (<http://dg.imp.kiev.ua/slinca>) on the basis of BOINC SZTAKI Desktop Grid (DG) technology [21, 22, 23].

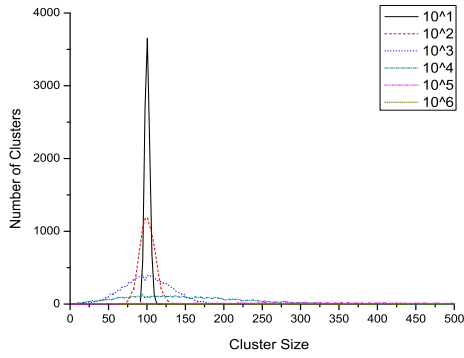
3.1. Pile-up — minimum active surface

The “pile-up” aggregation of monomers (see Fig. 1a) has a minimum active surface and was simulated under condition that $k_d \neq k_a$. The kinetics of rearrangements from the initial configuration is shown in Fig.4.

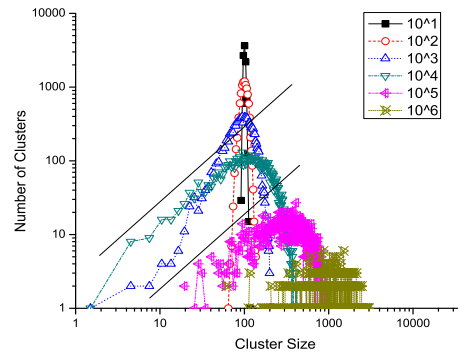
After some Monte Carlo sweeps (MCSs) of the initial configuration the broad peak appears, which corresponds to the average cluster size. The size distributions of pile-ups (Fig. 4a,b) become asymmetric, but they preserve their one-peak shapes. And their CDFs (Fig. 4c,d) demonstrate the “diffusive” scaling law, which becomes evident after some number of MCSs, namely after $t > 10^4$. It can be seen visually by the shift of the simulated CDFs to the right side (proportionally to \sqrt{t}) on the log-log plot in Fig. 4d and can be compared with the same shift of the analytically calculated CDFs in Fig. 3b. The two straight lines are given in Fig. 4b as a guide for eyes to emphasize that $f(n, t) \sim n$ for $n < n_0$ and $t > t_0$, that is follows from (5).

3.2. Wall — maximum active surface

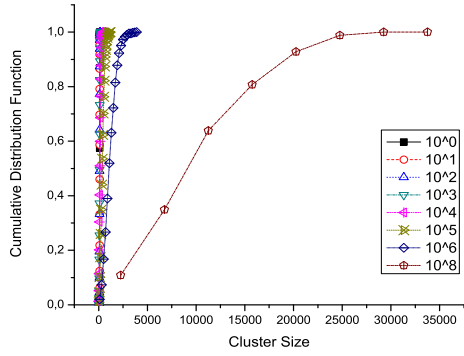
The “wall” aggregation of monomers (see Fig. 1b) has a maximum active surface and was simulated under the same condition that $k_d \neq k_a$. The kinetics of rearrangements from initial configurations is shown in Fig. 5. It can be seen that size distributions of walls (Fig. 5a,b) become asymmetric also. Moreover, they do *not* preserve their one-peak shapes after some number of MCSs and become scale-free, as it was predicted by the analytical solution



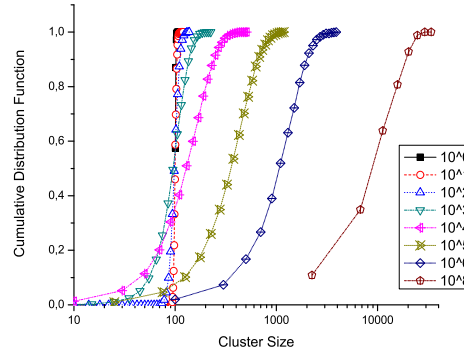
a)



b)



c)



d)

Figure 4: Size distributions of *pile-ups* for different stages of aggregation kinetics in: (a) linear and (b) double logarithmic coordinates (the straight lines are given as a guide for eyes to emphasize linear part of $f(n, t)$); and their cumulated distribution functions for: (c) linear and (d) logarithmic values of cluster size. Figures near symbols denote the number of Monte Carlo steps (MCSs).

(15) for $t > t_0$. After some Monte Carlo sweeps (MCSs) the initial peak, that corresponds to the initial cluster size n_0 , disappears and the scale-free distribution *without distinctive peak* appears. This transition is much more evident in the log-log representation of cluster size distributions on Fig. 5b. Their CDFs (Fig. 5c,d) also demonstrate the “linear” scaling law (17), which becomes evident after some number of MCSs, when the shift of CDFs to the right side of the plot in Fig. 5d becomes linearly proportional to t after $t > 10^2$. One can easily compare it with the similar shift of CDFs in Fig. 3b).

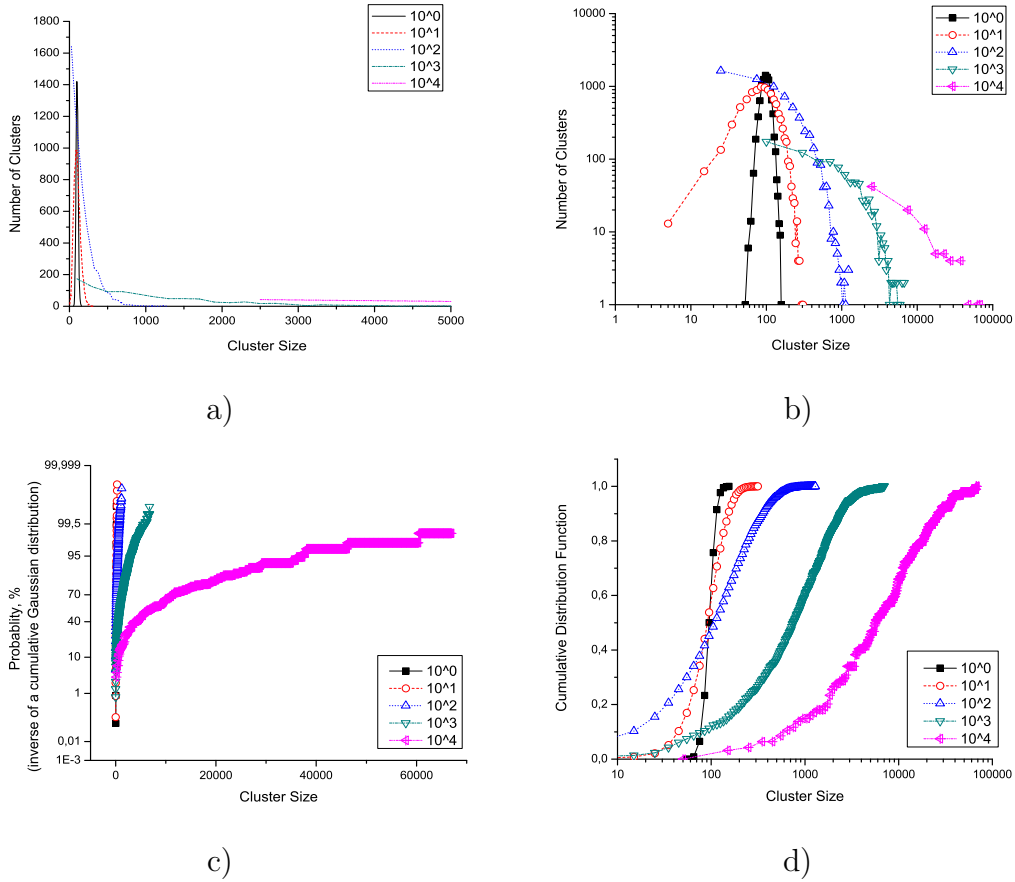


Figure 5: Size distributions of *walls* for different stages of aggregation kinetics in: (a) linear and (b) double logarithmic coordinates; and their cumulated distribution functions for: (c) linear and (d) logarithmic values of cluster size. Figures near symbols denote the number of MCSs.

4. Discussion of Results

Comparison of analytical and simulation results shows that monomer aggregation (at least, in pile-up and wall configurations of clusters) can be satisfactorily described by the proposed theoretical model of one-step aggregation processes. The important thing is that some scaling laws can be determined experimentally by scaling analysis of size distributions (and correspondent probability density functions — PDFs) and CDFs of the real aggregating ensembles. Below some attempts of such analysis are shown on the basis of aforementioned simulation results.

4.1. Pile-up — minimum active surface

The application of “infinite” diffusive scaling law (9) to simulated size distributions (Fig. 6a) and CDFs of pile-ups (Fig. 6b) shows the clear difference between two scaling regimes: “infinite” (9) and “semi-infinite” (10):

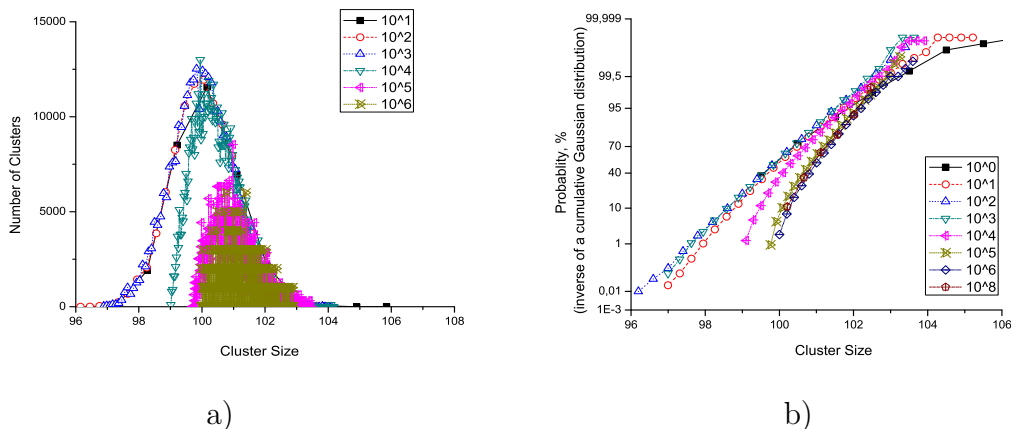


Figure 6: Different stages of aggregation kinetics of *pile-ups* represented by scaled: (a) size distributions and (b) cumulated distribution functions. Figures near symbols denote the number of MCSs.

- The “infinite” diffusive scaling law (9) corresponds to the initial stage $t < t_0$, i.e. the scaled size distribution curves are attracted to the initial symmetric size distribution; and the scaled CDF curves — to the initial *straight* line on probability plot in Fig. 6b (straight line on such plot corresponds to CDF of normally distributed values).

- The “semi-infinite” diffusive scaling law (10) takes place later (for $t > t_0$) after some transient period, i.e. the scaled size distribution curves are attracted to some other *asymmetric* size distribution; and the scaled CDF curves — to other *curved* line on probability plot in Fig. 6b.

The approximate transition region between two scaling laws can be observed in Fig. 6 as the solitary “water line” curve for $t = 10^4$ (denoted by down-directed triangles (∇) in Fig. 6a and by left-directed triangles (\triangleleft) in Fig. 6b), i.e. for the moment of the first-passage of a cluster through the point of disappearance ($n = 1$).

4.2. Wall — maximum active surface

The application of “infinite” diffusive scaling law (16) to simulated size distributions (Fig. 7a) and CDFs of walls (Fig. 8a) shows the other clear difference between two scaling regimes: “infinite” diffusive (16) and “semi-infinite” linear (17):

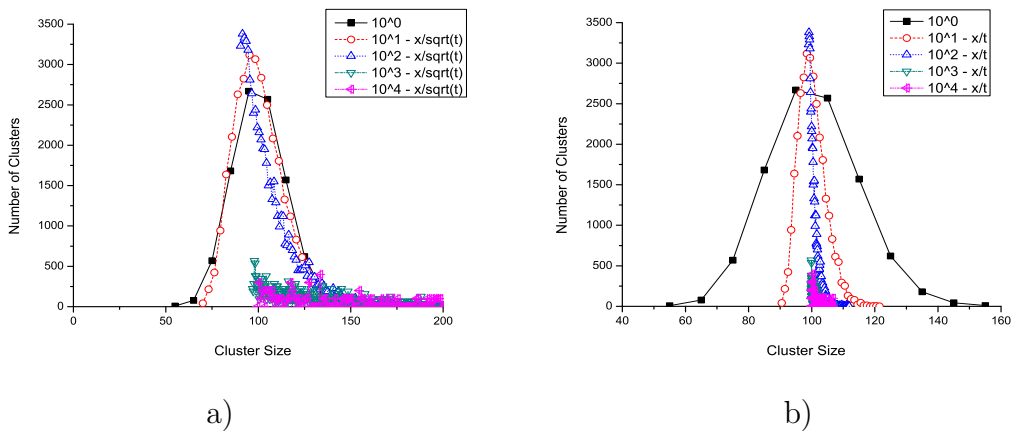


Figure 7: Wall size distributions for different stages of aggregation kinetics scaled by: (a) “infinite” diffusive scaling law (16); (b) “semi-infinite” linear scaling law (17). Figures near symbols denote the number of MCSs.

- The “infinite” diffusive scaling law (16) corresponds to the initial stage $t < t_0$, i.e. the scaled size distribution curves are attracted to the initial symmetric size distribution Fig. 7a; and the scaled CDF curves — to the initial *straight* line on probability plot in Fig. 8a.

- The “semi-infinite” linear scaling law (17) takes place later (for $t > t_0$) after some transient period, i.e. the scaled size distribution curves are attracted to some other *asymmetric* and *scale-free* size distribution (on Fig. 7b); and the scaled CDF curves — to other *curved* line on probability plot (Fig. 8b).

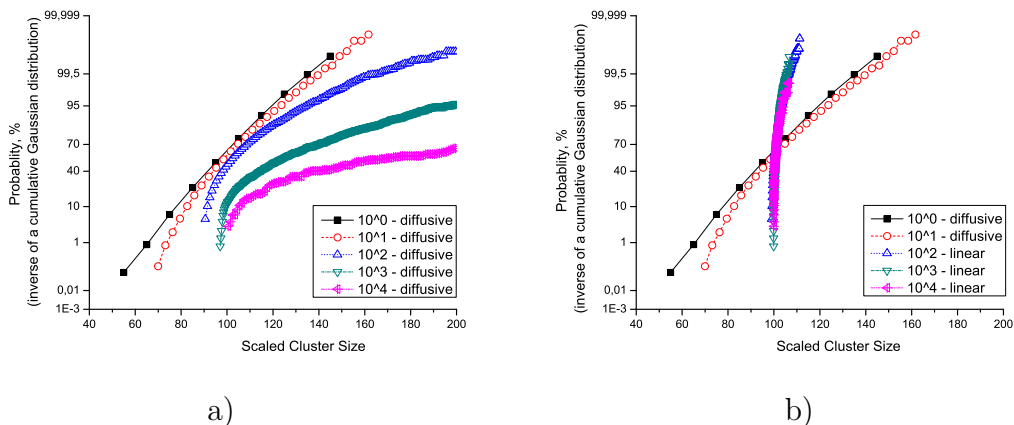


Figure 8: Scaled cumulated distribution functions for *walls* scaled by: (a) “infinite” diffusive scaling law (16); (b) mixed scaling laws — “infinite” diffusive (16) and “semi-infinite” linear (17) (see marks in legends of markers). Figures near symbols denote the number of MCSs.

The transition between two scaling laws can be clearly observed in Fig. 8b, where two family of collapsed curves are seen.

Scaling analysis of simulated (or experimentally obtained) size distributions (and PDFs) is very hard and prone to errors task, because of the some uncertainty related to proper and optimal binning procedures for preparation of histograms. In contrast, the scaling analysis of experimental and simulated CDFs has much higher stability to statistical deviations and outliers among data. The better collapse of scaled CDF curves could be seen even by visual comparison of scaled simulated histograms (Fig. 6a and Fig. 7a) with their scaled CDFs (Fig. 6b and Fig. 8b).

The initial “singular” configurations of walls after some time sweeps evolve to scale-free distributions (Fig. 7a), that is different from pile-up distributions with broad peaks for the same time (Fig. 6a). That is why in practical sense the notion of “average cluster size” seems to be meaningless for this kind of cluster size distributions (i.e. for exponential-like wall

arrangements) without distinctive peaks. This observations can give some insights as to possible roots for self-affine arrangements of defects and their manifestations at the surface of plastically deformed metals. Because in the asymptotic limit of high values of $n > n_0$ and $t \gg t_0$ the exponential distribution of wall sizes (15) can be approximated as $f(n, t) \sim A(t) - B(t)n$, where $A(t)$ and $B(t)$ are some functions of time steps. That is why in practice to estimate the level of hierarchy of defect substructures and related scale of damage it is necessary to measure not only the integral “averaged” characteristics of defect ensembles (density per area, average size, etc.), but also to define more specific characteristics, related with their size distribution, like CDFs and their parameters [24]. One of the examples of such scaling analysis applied for CDFs was demonstrated for statistical analysis of features observed on surfaces of plastically deformed Al single crystals under real-time video monitoring and processing [25].

At the moment some details of the simulation process cannot be compared directly with the theoretical results for large n and t because simulations were carried out for relatively low number of aggregating monomers ($\sim 10^6$) and in the limited time range ($< 10^4$ steps). That is why to check the exact solutions and make more reliable conclusions the bigger simulations are under way now in the DG DCI “SLinCA@Home”.

In the more general sense, scaling analysis of experimental distributions could allow us to determine their intrinsic symmetry and bring to light the corresponding aggregation scenario for many other applications related with aggregation phenomena, for example for investigation of city population dynamics [26].

5. Conclusions

The idealized general model of one-step processes to characterize aggregate growth was proposed that allowed us to find the scaling characteristics of some aggregation scenarios. Some factors that can cause scaling transition and appearance of the self-affine size distribution of the aggregating system of solitary agents (monomers) and their aggregates (clusters) were brought to light: the rate of monomer exchange between clusters, cluster geometry, and initial cluster size. It was shown that the simplified aggregate growth can be described by the one-variable Fokker-Planck equation in general form with time-independent drift and diffusion coefficients. In some aggregation scenarios it could be transformed to the equivalent equations, from which

the non-stationary analytical solutions with some initial and boundary conditions can be obtained.

Two primitive cases of cluster aggregation were considered analytically and simulated by Monte Carlo method to illustrate the different cluster distributions in different aggregation kinetics: model with *minimum* active surface (singularity) that corresponds to “pile-up” aggregation of dislocations, and model with *maximum* active surface that corresponds to “wall” aggregation of dislocations. It was shown that initial “singular” *symmetric* distribution of pile-ups evolves according to “infinite” diffusive scaling law and later it is replaced by the other “semi-infinite” diffusive scaling law with *asymmetric* distribution of pile-ups. In contrast, the initial “singular” *symmetric* distributions of walls initially evolve according to the diffusive scaling law and later it is replaced by the other linear scaling law with *scale-free* exponential distributions without distinctive peaks.

From the practical point of view and in the more general sense, the scaling analysis of experimental distributions of aggregating monomers and clusters will allow to determine their intrinsic symmetry, bring to light the corresponding aggregation scenario, and influence of aforementioned parameters (rate of monomer exchange between clusters, cluster geometry, and initial cluster size).

6. Acknowledgements

The work presented here was partially funded by the FP7 DEGISCO (Desktop Grids for International Scientific Collaboration) (<http://degisco.eu>) project, which is supported by the FP7 Capacities Programme under grant agreement number RI-261561.

References

- [1] B. Mandelbrot, Nature 308 (1984) 721.
- [2] S. Stach, J. Cybo, Mater. Charact. 51 (2003) 79,87.
- [3] Y. Gordienko, E. Zasimchuk, Proc. SPIE 2361 (1994) 312.
- [4] E. Zasimchuk, Y. Gordienko, R. Gontareva, I. Zasimchuk, J.Mater. Eng. and Perf. 12 (2003) 68.
- [5] Y. Gordienko, Adv. Eng. Mater. 8 (10) (2006) 957.

- [6] T. Kleiser, M. Bocek, *Z. Metallkunde* 77 (1986) 587.
- [7] H. Neuhäuser, *Solid State Phenomenon* 3 & 4 (1988) 407.
- [8] M. Zaiser, F. Grasset, V. Koutsos, E. Aifantis, *Phys. Rev. Lett.* 93 (2004) 195507.
- [9] P. Hähner, K. Bay, M. Zaiser, *Phys. Rev. Lett.* 81 (1998) 2470.
- [10] G. Ananthakrishna, *Physics Reports* 440 (2007) 113.
- [11] I. Lifshitz, V. Slyozov, *Zh. Eksp. Teor. Fiz.* 35 (479).
- [12] I. Lifshitz, V. Slyozov, *Sov. Phys. JETP* 8 (331).
- [13] A. Zangwill, *Physics at Surfaces*, Cambridge University Press, New York, 1988.
- [14] S. Chandrasekhar, *Rev. Mod. Phys.* 15 (1943) 1.
- [15] S. Ispolatov, P. Krapivsky, S. Redner, *Eur. Phys. J. B* 2 (1998) 267.
- [16] F. Leyvraz, S. Redner, *Phys. Rev. Lett.* 88 (2002) 068301.
- [17] N. G. van Kampen, *Stochastic processes in physics and chemistry*, North-Holland, Amsterdam, 1981.
- [18] A. Fokker, *Ann. Phys.* 43 (1914) 810.
- [19] M. Planck, *Preuss. Akad. Wiss. Phys. Math. K1* (1917) 325.
- [20] Y. Gordienko, *Phys. Rev. Lett.*, submitted.
- [21] P. Kacsuk, J. Kovács, Z. Farkas, A. Marosi, G. Gombás, Z. Balaton, *Journal of Grid Computing* 7 (4) (2009) 439.
- [22] E. Urbach, P. Kacsuk, Z. Farkas, G. Fedak, G. Kecskeméti, O. Lodygensky, A. Marosi, Z. B. G. Caillat, G. Gombás, A. Kornafeld, J. Kovács, H. He, R. Lovas, *Journal of Grid Computing* 7 (3) (2009) 335.
- [23] Z. Balaton, G. Gombas, P. Kacsuk, A. Kornafeld, J. Kovacs, A. Marosi, G. Vida, N. Podhorszki, T. Kiss, in: *Proc. of the 21th Int. Parallel and Distributed Processing Symposium*, Long Beach and California, USA, 2007, p. 1.

- [24] O. Gatsenko, O. Baskova, Y. Gordienko, in: Proc. of Cracow Grid Workshop (CGW'09), Cracow, Poland, 2010, p. 264.
- [25] O. Gatsenko, O. Baskova, O. Lodygensky, G. Fedak, Y. Gordienko, Key Engineering Materials 465 (2011) 306.
- [26] O. Gatsenko, O. Baskova, Y. Gordienko, in: Proc. of Cracow Grid Workshop (CGW'10), Cracow, Poland, 2011, in print.